

Geotechnical behaviour of nano-silica stabilized organic soil

Govindarajan Kannan^a and Evangelin Ramani Sujatha*

Centre for Advanced Research in Environment, School of Civil Engineering, SASTRA Deemed to be University,
Thirumalaisamudram, Thanjavur - 613401, Tamil Nadu, India

(Received May 14, 2021, Revised November 4, 2021, Accepted December 1, 2021)

Abstract. Suitable techniques to stabilize organic soil and improve its engineering behaviour are in demand. Despite various alternatives, nano-additives proved to be an effective stabilizer owing to their strength enhancing properties. The study focuses on using nano-silica as a potential stabilizer to improve organic silt. Soil was treated with four dosages of nano-silica namely 0.2%, 0.4%, 0.6% and 0.8% of dry weight of the soil. Nano-silica treated soil showed a strength increase of nearly 25% at a dosage of 0.4% after curing for two hours. Strength of the treated soil improved with age. Strength improved by nearly 62.9% after 28 days of curing and 221.4% after 180 days of curing due to formation of Calcium – Silicate – Hydrate (CSH) gel in the soil matrix. Dosage of 0.6% nano-silica is observed to be the optimum dosage. Coefficient of permeability and compression index showed an increase by 13.32 and 5.5 times respectively owing to aggregation of particles and creation of void spaces as visualized from the scanning electron micrographs. Further model foundation study and numerical parametric studies using PLAXIS 2D indicate that optimized and economic results can be obtained by varying the additive dosage with depth.

Keywords: consolidation; model study; nano-silica; organic silt, permeability; strength, surface roughness

1. Introduction

Rapid increase in the need for construction spaces has imposed a severe restriction on the choice of soil with favorable geotechnical properties. Soil previously deemed not suitable for construction activities like highly plastic clay, expansive soil, organic soil and collapsible soils, etc. therefore need to be improved suitably to support these activities. Among them, soils with organic content are generally considered highly incongruous for construction activities due to their low strength and high compressibility. Numerous techniques like stabilization, preloading, grouting and reinforcement, etc. are used to improve the properties of the soil. Stabilization is the most common and popular method adopted for ground improvement. Cementitious material like lime (Rastegarnia *et al.* 2020), cement (Shooshpasha and Shirvani 2015), and fly ash (Mohanty *et al.* 2017) are the conventional stabilizing materials used in the field. The addition of cementitious materials improves the strength and deformation response of the treated soil in addition to modifying the compressibility behaviour of the soil (Bahmani *et al.* 2014). Filler materials like rice husk ash (Gupta and Kumar 2017), groundnut shell ash (Folagbade and George 2010), brick powder (Hidalgo *et al.* 2019), etc. are also used for improving the properties of the soil. Sakr *et al.* (2009) used lime to improve the behaviour of clay with organic content and reported that addition of 7% lime improved the strength

by 6.6 times through the formation of new cementitious products. Bobet *et al.* (2011) attempted to study the consolidation behaviour of cement treated highly organic soil and found that the inclusion of cement not only increased the effective stress that the soil can withstand but also the coefficient of consolidation of the soil. Tasthan *et al.* (2011) used fly ash to stabilize organic soil and found that the pozzolanic action led to strength improvement, however strength reduced exponentially with an increase in organic content. The choice of these material for ground improvement suffers serious limitations as it permanently modifies the soil environment. Also, material like cement, a widely used additive used for soil stabilization results in emission of greenhouse gases like carbon dioxide, nitrogen dioxide and sulfur dioxide causing air pollution and climate change. Stabilizing soil with fly ash renders the soil matrix granular and increases its water absorption capacity (Tejasvi and Kumar 2012). The energy and environmental concerns raised by the conventional stabilizers underline the need for an effective stabilizer which also needs to be economic for improving the soil properties.

Nano-materials offer an attractive alternative to conventional materials in many fields of construction engineering. Nano-materials have been effective in improving the strength of concrete (Norhasri *et al.* 2017), yields stronger structural composites (Saloma *et al.* 2015), and improved surface and thermal properties (Sikora *et al.* 2018). Nano sensors find extensive application in monitoring the health and safety of structural elements (Karthick *et al.* 2019). Nano technology also finds varied applications in water treatment and environmental engineering (Qu *et al.* 2013). Nanoparticles owing to their size have a high specific surface and therefore interact readily with soil particles (Ghasabkolaei *et al.* 2017). The

*Corresponding author, Professor

E-mail: r.evangelin@gmail.com; sujatha@civil.sastra.edu

^aResearch Scholar

use of nano-materials for geotechnical applications though are limited. The effectiveness of nano-particles in stabilizing soil depends on several factors like the purity of selected nano-material, temperature, type of soil and the experimental conditions selected for the study (Changizi and Haddad 2017). Literature review points out that materials like nano clay (Taha and Taha 2012, Tabarsa *et al.* 2018), nano-silica (Changizi and Haddad 2017), nano carbon fibers (Alsharif *et al.* 2016), nano magnesium oxide (Gao *et al.* 2018), nano calcium carbonate (Choobbasti *et al.* 2019) nano alumina (Taha and Taha 2012), and carbon nanotube (Alsharif *et al.* 2016), chemical based nano stabilizers like terrasil and zycobond (Bahrami *et al.* 2020) etc. are used as nano-additives for soil stabilization. Though the studies show promising results, transfer of this technology to field applications need further research augmenting its advantages and new ways for field technology transfer.

Nano-clay increased the plasticity index (Kananizadeh *et al.* 2011, Tabarsa *et al.* 2018) and the compressive strength of clay (Tabarsa *et al.* 2018) but decreased its permeability (Kananizadeh *et al.* 2011). Bahmani *et al.* (2014, 2016) and Ghasabkolaei *et al.* (2016) studied the performance of cement-treated clays along with nano-silica. The authors indicated that nano-silica treatment enhances the performance of cement-treated soil. Changizi and Haddad (2015) analyzed the outcome of soil stabilized with nano-silica and recycled polyester fiber in soft clays. The results pointed out that nano-silica could help reduce failure strain, and this nano-silica – fiber combination improved the soil's strength, particularly the post-peak behaviour. Changizi and Haddad (2017) studied the performance of two different clays (high plastic and low plastic clays) and verified the formation of viscous gel in the soil-additive mass; also, they identified the optimum nano-silica content as 0.7%. Ahmadi and Shafiee (2019) compared the influence of micro-silica and nano-silica in clayey soil and observed that soil showed better performance at comparatively lower nano-silica dosages of 1%. Ghadr *et al.* (2020) stabilized peat with colloidal nano-silica and reported that a colloidal solution with 15 to 20% nano-silica would offer better improvement in strength and reduced the strain at failure with a brittle stress-strain behaviour. Results of experimental investigations reported by several authors (Bahmani *et al.* 2014, Ghasabkolaei *et al.* 2016) indicated that nano-silica as an activator in cement-treated soils significantly influences clay's strength. Nano-silica exhibits enhanced pozzolanic activity because of the presence of large amount of pure amorphous silica (Buazar 2019) and improves the density of the treated soil due to void filling (Choobbasti and Kutanaei 2017, Thomas and Rangaswamy 2020). The increase in density is caused by mechanisms like nucleation effect where the soil particles are enveloped by hydration products (Lv *et al.* 2018). The physical and chemical changes caused by nano-silica addition led to nearly 20 % increase in the strength of these cementitious composites (Bahmani *et al.* 2014). Shahsavani *et al.* (2020) reported that addition of 0.5% nano-silica and industrial waste reduced the swelling potential of the soil by 29.54%. Nano-alumina was used to stabilize clay in conjunction with

sewage sludge ash and resulted in an increase of strength by nearly 4.2 folds (Luo *et al.* 2012). Similarly, nano magnesium oxide enhanced the strength of the clay soil by reduction in pore size (Ahmadi 2019). Taha and Ying (2010) observed that addition of carbon nanotubes for improving soil resulted in the increase of plasticity index by 22% and compression index by 32% while reported a reduction in the permeability of the treated soil. Nano calcium carbonate resulted in the increase of unconfined compressive strength by around 66% by the formation of adhesive gel (Choobbasti *et al.* 2019). Nano-clay and nano-silica are easily available for commercial applications and therefore are often selected as additive for ground improvement. Nanomaterials like colloidal silica and nano-clay caused a reduction in the permeability of the clay soil due to pore filling (Gallagher *et al.* 2007; Kananizadeh *et al.* 2011, Tabarsa *et al.* 2018, Wong *et al.* 2018). Authors Taha and Ying (2010) reported that the use of carbon nanotubes in clay soil resulted in the increase in compressibility of the soil. Changizi and Haddad (2017) observed that nano-silica stabilization controlled the settlement of soft clay.

In addition to strength improvement studies, Changizi and Haddad (2017) have also attempted to study the consolidation behaviour of nano-silica treated soil through one dimensional consolidation tests. Results indicated that the compression index of 0.7% treated soil showed a reduction by 0.4 times and the pre-consolidation pressure improved by 3.28 times for soft clay. The authors claimed that viscous gel formation led to improved performance on treated soil. Reported literatures supported their results with observations from X-Ray Diffraction (XRD), Scanning Electron Microscope (SEM) and Fourier Transform Infrared Spectroscopy (FTIR) reports to emphasize the physical and chemical changes upon treatment (Krishnan and Shukla 2019). Changizi and Haddad (2017) reported the formation of viscous gel through Field Emission Scanning Electron Microscope (FESEM), however they suggested that adding water to soil and nano-silica mix didn't initiate any chemical reaction by comparing the plots of XRD analysis. Contrary to Changizi and Haddad (2020), Ahmadi and Shafiee (2019), suggested that no gel was formed as an outcome of nano-silica treatment of soil, and suggested that strength improvement was only the effect of pore filling mechanism of nano-silica in between soil particles. Lv *et al.* (2018) reported that addition of nano-silica induced the formation of C-S-H (Calcium Silicate Hydrate) and C-A-S-H (Calcium Aluminate Silicate Hydrate) gels on loess and confirmed their results through FTIR patterns. Hence, it is evident that strength improvement and the nature of strength improvement depends on type of soil to a great extent.

Several studies have been conducted on the use of nano-silica as an activator for a soil stabilized with a cementitious material. Cementitious material required for soil stabilization depends on the soil type. As per the reports of American Concrete Institute, cement stabilization is not suitable for soil with organic content greater than 2% (Firoozi *et al.* 2017). Large quantities of cementitious material are required to stabilize soil with organic content

and therefore is not an economic option. Literatures reported on the usage of nano-silica for stabilization of organic soil are scarce and requires a detailed investigation to establish nano-silica as potential stabilizer for soil with organic content. This study explores the possibility of using nano-silica as a soil stabilizer without a cementitious base like lime or cement for improving the properties of a silty soil with moderate organic content. The study intends to address the issues raised by the permanent modification of soil environment on addition of cementitious materials and offer an economic solution. The significance of the study is that it attempts to use nano-silica as a stand-alone stabilizer rather than using it as an activator for cement stabilization. Nano-silica is used in small dosages of 0.2%, 0.4%, 0.6% and 0.8% of dry weight of soil and its effect on geotechnical properties like consistency limits, compaction characteristics, deformation behaviour, strength, permeability and compressibility are investigated. Element analysis through XRD and FTIR techniques was used to infer the changes in the mineralogy of the soil treated with nano-silica. Micrographs from scanning electron microscope (SEM) are used to understand the morphological changes and mechanism of strength gain. SEM micrographs were also used to ascertain the pore size and surface roughness of the treated soil. Further model studies on untreated soil and nano-silica treated soil were conducted followed by numerical parametric analysis to identify the optimum depth for stabilization in field. Results indicates that the choice of nano-silica significantly reduces the material costs involved in soil stabilization. Also, this provides an energy efficient and sustainable alternative to soils stabilized with cementitious base.

2. Materials

2.1 Soil

Soil was collected from Ariyalur District in Tamil Nadu, India for this investigation. The soil was extracted from trenches 1 m deep to avoid loose unaggregated topsoil and organic material. Soil is classified as organic silt (OL) as per the Unified Soil Classification System (USCS) (ASTM D2487 (2017)). Table 1 lists the soil properties.

2.2 Nano-silica

Nano-silica was procured from Astrra Chemicals, Chennai, Tamil Nadu. The supplier specified properties of nano-silica are presented in Table 2. The average size of the nano-silica particles used for the study is 17 nm. It can be inferred from Table 2 that 99.88% of the nano-silica comprised of silicon dioxide. Nearly 0.06 % of carbon was present in the procured nano-silica. Traces of chlorides, alumina, titanium oxide, and ferrous oxide were also present.

3. Methodology

3.1 Preparation of soil samples

Table 1 Properties of the black soil

Soil properties	Values
Liquid limit (%)	48.8
Plastic limit (%)	26.3
Shrinkage limit (%)	5.3
Plasticity index (%)	22.5
Specific gravity	2.3
Differential free swell index (%)	35
Organic material (%)	13.6
Gravel (%)	2
Sand (%)	25
Silt (%)	52
Clay (%)	21
Classification (USCS)	OL (Organic silt)

Table 2 Properties of the nano-silica

Properties	Values
Particle size (nm)	17
Specific surface area (m ² /g)	202
Tamped Density (g/L)	44
pH	4.12
SiO ₂ (%)	99.88
Carbon (%)	0.06

The soil was sun-dried, rrammed, and pulverized. Pebbles and dry twigs were removed from the soil during the process to ensure homogeneity in the soil content. The soil was sieved for different particle sizes as required for various experiments. The dosage of nano-silica was ascertained based on literature studies and trial studies at the start of the experimental investigation. The required amount of nano-silica (0.2%, 0.4%, 0.6%, and 0.8% by dry weight of soil) was weighed, and hand-mixed with the soil to ensure uniform mixing nanomaterial with the soil. The soil sample was mixed thoroughly with a dry spatula through the entire process as the nano-silica was added to the soil in small instalments.

3.2 Experimental investigation

The organic content and swelling nature of the soil were ascertained using loss on ignition and differential free swell index tests as per the guidelines of ASTM D2974 (2020) and ASTM D5890 (2019) respectively. Liquid, plastic, and shrinkage limit tests were conducted adhering to the standards of ASTM D4318 (2017) and ASTM D427 (2004), respectively. Compaction tests were performed on untreated soil, and nano-silica treated soil samples to ascertain their maximum dry unit weight (MDD) and optimum moisture content (OMC). Nano-silica – soil mixture was initially sprayed with 10% of water by dry weight of soil and mixed thoroughly. The soil – nano-silica blends were stored in air-tight covers for 12 hours to promote the reaction between water, soil and nano-silica. Then nano-silica – soil mixture

was compacted with a compaction effort equal to that of light compaction as per the guidelines of ASTM D698 (2012). Unconfined compressive strength (UCS) test was performed on soil mixed with different dosages of nano-silica sprayed with water equivalent to its OMC. The sample was mixed thoroughly and compacted into cylinders of diameter 38 mm and height 76 mm. The prepared samples were stored in air-tight covers for curing without losing its moisture content.

UCS tests were carried out for five different curing periods, namely 0, 7, 14, 28 and 180 days on nano-silica treated soil as per ASTM D2166 / D2166M (2016). The 0-day test was conducted after two hours of sample preparation and was considered the sample's initial strength. Permeability and consolidation tests were conducted on organic soil following the standards of ASTM D5856 (2015) and ASTM D2435 / D2435M (2020), respectively. One-dimensional consolidation test was carried out on selected dosages of nano-silica treated samples (i.e.,) 0.6 % and 0.8 %.

SEM, XRD and FTIR analyses were conducted to understand the mechanism involved in nano-silica treated soil's behavioral aspects. SEM micrographs was obtained using Tescan Vega 3 instrument to understand the influence of nano-silica treatment on porosity and surface roughness of nano-silica treated soil samples. Chemical compounds present in the treated and untreated samples were identified using Bruker XRD instrument for a 2θ range of 20° to 80° . The variation of functional groups and formation of new bonds were analysed using Perkin Elmer FTIR spectrometer for wavenumber between 400 cm^{-1} and 4000 cm^{-1} .

Image processing of SEM micrographs was carried out using Matlab R2020a adopting the procedure outlined by Rabbani *et al.* (2017). It is based on the assumption that the darker regions of the SEM images imply deeper surfaces such as pore spaces (Rabbani and Salehi 2017, Ezeakacha *et al.* 2018). The procedure involves intensity mapping followed by binary segmentation, where the darker regions are shown against a white background. The pore spaces are then represented in different colour combinations. Although the method is approximate, this serves as a quantitative indicator of the range of porosity and pore space in the soil matrix. Likewise, surface roughness was measured using Gwyddion 2.56 software, which uses an indirect image profilometry technique on the SEM images to identify the roughness coefficients (Pavlović *et al.* 2012).

3.2 Model study

To analyse the practical feasibility and foundation behaviour on nano-silica treated soil, model analysis was conducted on untreated soil and soil treated with 0.6% nano-silica. A circular tank with diameter 270 mm and height 320 mm was used for the study. A similar kind of tank was used by Ali and Abbas (2019) for their study on screw pile in soft clay. Test soil mixed with water at optimum moisture content was stored in an airtight box for 7 days to facilitate uniform spreading of moisture (Dash *et al.* 2003) and to promote the reaction between soil and

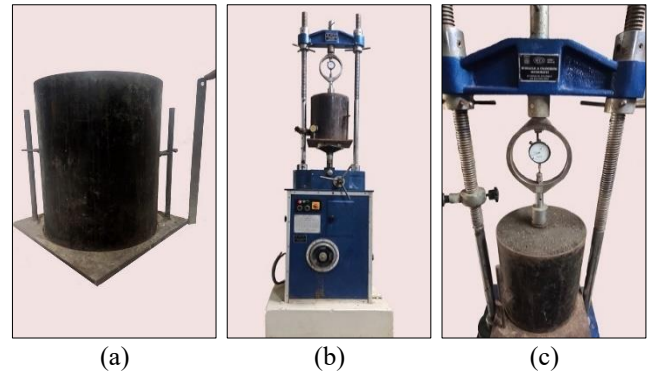


Fig. 1 (a) Tank for the model study (b) Experimental setup for model study and (c) model footing arrangement in test tank

nano-silica in treated soil. Then the test tank is filled with soil at its maximum dry unit weight in 8 layers with each layer being 4 cm. Each layer was tamped until required density is achieved. Circular mild steel plate with diameter 50 mm and thickness 5 mm was used to simulate a rigid circular footing behaviour. The diameter of the model footing was selected such that it adheres to the guidelines of ASTM D1194 (1994) with plate size greater than four times the test area size. The test was conducted on a loading frame (Sadoglu *et al.* 2009) until failure at a strain rate of 1.25 mm/minute until the plate completely penetrated into the soil. Fig. 1 represents the experimental set-up used for model analysis and the placement of footing over the test tank.

3.3 Parametric study

Using same dosage of additive for the entire depth of stabilisation would yield an uneconomical stabilisation result. Hence, considering the fact that intensity of additional pressure decreases with depth, the dosage of nano-silica is varied with different layers. Prior to the parametric study, the model study was validated with PLAXIS 2D to identify the nature of actual vs. software predicted curves. The parametric analysis was conducted using axisymmetric loading condition and 15 noded elements with a medium sized mesh. Axisymmetric condition was considered to reduce the complexity of mesh development and to reduce the computational time and effort. The parametric analysis was carried out for three different footing sizes to ensure uniformity in the observed trend. The footing sizes considered for the study are 1.2 m, 1.5 m and 1.8 m and stabilisation was done upto a depth of 3 m below the base of footing. To simulate a condition similar to model study, the boundary to footing dimension ratio in parametric study was maintained same as model study. Mohr-coulomb material model with drained soil behaviour was selected to simulate the behaviour of soil. Loading is done with prescribed displacement condition to simulate rigid footing behaviour. All the input parameters are taken from the experimental results and strength parameters are taken from the results of 7 days curing, considering it to be an optimal time one can wait after

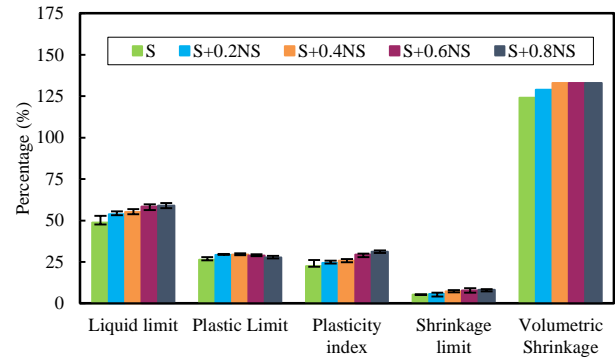
stabilising the ground, prior to the start of construction activities.

4. Results and discussions

4.1 Effect of nano-silica on the plastic behaviour

Nano-silica tends to modify the plastic nature of the soil to a small degree. The liquid limit of the soil increases marginally from 48.8% for untreated soil to nearly 59% at dosage of 0.8% nano-silica. The liquid limit increased by 20.9% for maximum nano-silica dosage investigated. Similar behaviour was reported by authors Bahmani *et al.* (2014) on adding nano-silica as an activator with cemented soil. The increase in liquid limit can be ascribed to the high specific surface area (SSA) of nano-silica (Erzin and Gunes 2013) that causes the treated soil to absorb more water resulting in a higher liquid limit. The plastic limit of the untreated soil is 26.3%. It increased to a maximum of 29.37% for 0.4% nano-silica treated soil. Further increase in nano-silica dosage showed a slight reduction in the plastic limit of soil. The plasticity index of the soil, which represents the range of water content in which the soil exhibits plastic behaviour also increases with the increase in nano-silica dosage from 22.5% for soil to 31.24% for 0.8% nano-silica dosage as observed from Fig. 2. An increase of 38.84% plasticity index is observed for the highest dosage of nano-silica investigated. The rise in plasticity index reflects the marginal change in plastic nature of the stabilized soil. Nano materials like nano-clay and carbon nano-tubes also causes a similar response in treated soil (Ghazi *et al.* 2011, Taha and Ying 2010). The change in plastic nature of the treated soil is a function of the soil type, type of clay minerals present and experimental procedure adopted.

The shrinkage limit is yet another measure that pertains to the plastic behaviour of the soil. The shrinkage limit of the soil as observed from Fig. 2 shows that it increases marginally with nano-silica dosage but tends to converge at higher dosages of 0.6% and 0.8%. The maximum increase in the shrinkage limit of the nano-silica treated soil in this study is 55.22%. The aggregation promoted by nano-silica leads to the development of void spaces, causing a reduction in density and volume of the dehydrated soil. On drying, generally, capillary suction increases owing to the increase in the capillary meniscus which causes an increase in the effective stress in the clay matrix leading to the volume change of the clay layer (Changizi and Haddad 2017). A corresponding increase in volumetric shrinkage, defined as the ratio between change in volume to original dry volume is also observed with the increase in nano-silica dosage. The volumetric shrinkage for untreated soil is 124% which increased significantly to a maximum of 133% for 0.4% treated soil and maintained a constant value for further dosages. Fig. 3 depicts the shrinkage cracks on the soil pat upon oven drying which explains the volumetric shrinkage experienced by the soil. This increased volumetric shrinkage could be due to increased plastic nature of treated soil as observed through plasticity index.



S: Soil; NS: Nano-silica

Fig. 2 Atterberg's limits plot for varying dosages of nano-silica

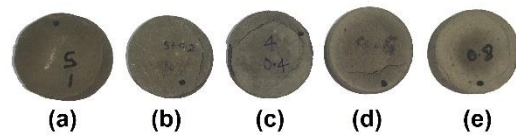


Fig. 3 Shrinkage pats (a) S (b) S+0.2NS (c) S+0.4NS (d) S+0.6NS (e) S+0.8NS

4.2 Compaction behaviour of nano-silica treated soil

The compaction curves of soil treated with nano-silica show a shift towards the left in the downward direction indicating a decrease in both the MDD and OMC of the treated soil. It can also be seen from Fig. 4 that the change in OMC is appreciable whereas the change is extremely marginal in the case of MDD. The soil selected for this study had a MDD of 16.8 kN/m³ and on the addition of the least dosage of nano-silica investigated (i.e.,) 0.2%, it reduced to 16.4 kN/m³. On further addition of nano-silica MDD decreased to 16.1 kN/m³ at 0.8% nano-silica dosage. It showed a reduction of nearly 4.17% at 0.8% nano-silica dosage. Fig. 4 also indicates that MDD tends to converge at higher dosage of nano-silica.

The decrease in MDD though very slight can be attributed to the aggregation of clay particles in the soil

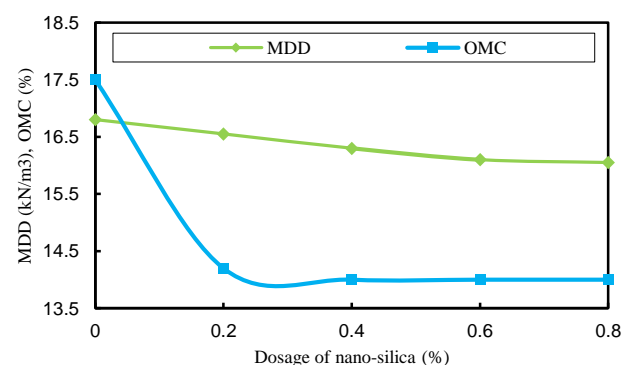


Fig. 4 MDD and OMC for varying dosages of nano-silica

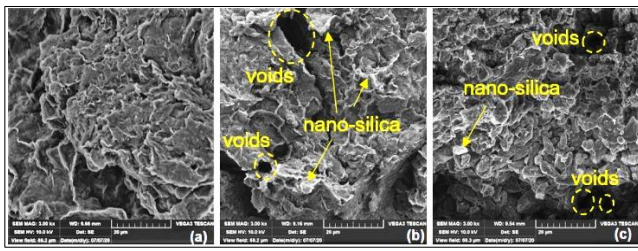


Fig. 5 SEM micrographs for varying dosages of nano-silica (a) Soil (b) Soil + 0.6% (0 day) (c) Soil + 0.8% (0day)

promoted by nano-silica and creation of void spaces in the soil matrix. Fig. 5 shows the micrographs of virgin soil and soil treated with 0.6% and 0.8% of nano-silica obtained using SEM at 0-day curing period (i.e.,) two hours after blending the soil with nano-silica. The images indicate that initially, the untreated soil had a dispersed structure (Fig. 5(a)). Addition of nano-silica tends to induce flocculation of the soil particles resulting in void spaces as observed from Figs. 5(b) and 5(c). The nano-silica coating on the soil is envisaged as white patches in Figs. 5(b) and 5(c).

The OMC of the soil is 17.5% and on addition of 0.2% nano-silica it reduced to 14.2%. On increasing the nano-silica dosage further, the OMC converged at 14%. The decrease in OMC can be ascribed to the usage of water for the hydration reactions in the soil matrix. The results of authors Changizi and Haddad (2017) and Bahmani *et al.* (2014) report a rise in OMC with the addition of nano-silica. The difference in the trend of change in OMC can be because of the procedure adopted for the study. In this study, the prepared soil samples are allowed to hydrate for 12 hours after blending the soil with nano-silica.

4.3 Deformation and Strength Behaviour of nano-silica stabilized soil

The stress-strain response for different dosages of nano-silica at various periods of curing is shown in Fig. 6. In general, it was observed that the nano-silica blending improved the strength of the soil and modified the soil's nature to a brittle nature with passage of time (Changizi and Haddad 2017, Ahmadi and Shafiee 2019, Ghadr *et al.* 2020). The untreated soil experienced failure with bulging, however with the nano-silica treatment, vertical cracks developed during failure indicating a brittle nature. As a result of nano-silica addition, the stress-strain behaviour of nano-silica treated soil showed distinct peak with definite failure load as shown in Fig. 6.

A similar pattern in deformation behaviour is observed with ageing also. Rapid reduction in post-peak strength is also observed in nano-silica treated soils compared to the gradual decrease of post-peak strength in untreated soil. Ghazavi and Bolhasani (2010) also reported a similar behaviour of sharp peak and drastic reduction in post peak strength on treating the clay soil with nano-silica. The shift from plastic to brittle behaviour is also observed on treating clay soil with other nano-materials like nano calcium carbonate (Choobasti *et al.* 2019), nano carbons (Taha *et al.* 2018) and colloidal silica (Ghadr *et al.* 2020) etc.

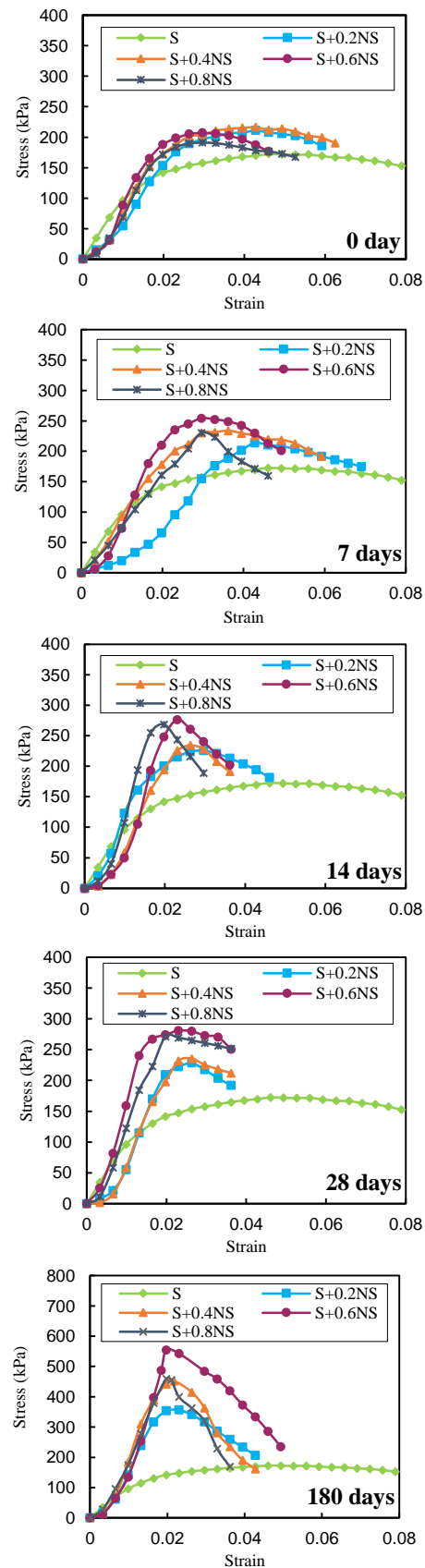


Fig. 6 Stress-strain plots of nano-silica treated soil for varying curing periods

Table 3 Failure strain: effect of curing period at different dosages of nano-silica

Dosage	0 day	7 days	14 days	28 days	180 days
S+0.2NS	0.0428	0.0428	0.0296	0.0263	0.0230
S+0.4NS	0.0428	0.0362	0.0263	0.0263	0.0217
S+0.6NS	0.0296	0.0296	0.0230	0.0230	0.0197
S+0.8NS	0.0296	0.0296	0.0197	0.0197	0.0197

Table 4 Failure modulus at various curing period and dosages of nano-silica

Dosage	0 day	7 days	14 days	28 days	180 days
S+0.2NS	4934.4	4993.6	7630.1	8678.1	15505.6
S+0.4NS	5052.7	6458.9	8906.4	8939.1	20829.5
S+0.6NS	6994.0	8583.9	12008.9	12196.1	28129.9
S+0.8NS	6445.1	7774.6	13619.7	13750.9	23341.6

The strain at failure for the various dosages of nano-silica and different curing periods are shown in Table 3. The nano-silica treated soil tends to resist higher loads at smaller strains (Fig. 6) and the failure strain decreases with the increase in nano-silica dosage (Changizi and Haddad 2015, 2017, Ahmadi and Shafiee 2019). Similar trend is also observed with increase in the curing period. For example, the virgin soil failed at a strain of 4.61% but the soil treated with 0.8% of nano-silica failed at a strain of 1.97%, much lower than untreated soil. This trend remained constant for all dosages of nano-silica during all the investigated curing periods. Failure strain of 0.8% nano-silica treated soil reduced to 35.7% after 0 and 7 days of curing, 57.1% after 14, 28 and 180 days of curing.

Adding nano-silica to the soil resulted in the formation of gel that resists the movement of the particles within the soil matrix. The resistance offered by the soil-gel matrix leads to the failure of the soil at lower strain. Table 3 indicates that at higher dosages (i.e.,) 0.4%, 0.6%, and 0.8%, the failure strain converged after longer curing periods (i.e.,) at 14, 28 and 180 days of curing. The deformation response of nano-silica treated soil shows similarity with the soil treated with other cementitious material like cement and lime (Bahmani *et al.* 2014).

The nano-silica treated soil's stiffness is measured in terms of secant modulus at failure load (failure modulus henceforth). The failure modulus (E) of the untreated soil is 3744 kPa. Table 4 presents the failure modulus of the organic soil treated with different nano-silica dosages at various curing periods. The failure modulus displayed an increasing trend, both with the nano-silica content and the curing period. Soil treated with 0.6% of nano-silica showed greater stiffness during earlier days of curing. At longer curing periods of 14, 28 and 180 days, stiffness was greater at a higher dosage of 0.8%. Soil cured for 180 days showed a maximum stiffness with an increase by 3.1, 4.6, 6.5, and 5.2 times the failure modulus of an untreated soil at the dosages of 0.2%, 0.4%, 0.6%, and 0.8% of nano-silica, respectively. The inclusion of nano-silica allows the soil to withstand more load per unit deformation; in other words, it

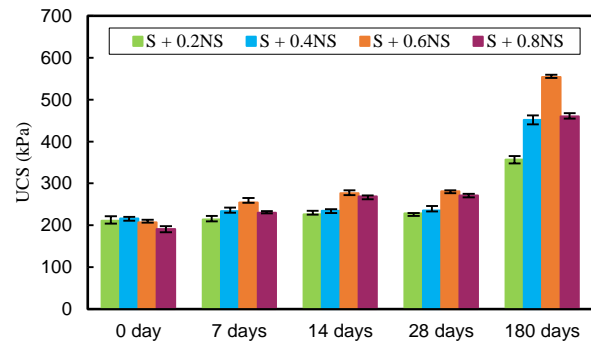


Fig. 7 Variation of UCS with curing periods at different dosages of nano-silica

increased its stiffness. Thus, the increased deformation modulus reflects the effect of failure at higher load and lower strain in the nano-silica treated soil samples.

Fig. 7 presents the modification in UCS of the soil treated with nano-silica at different dosages and curing periods. The strength of the organic soil was 172.4 kPa. The initial testing at 0-day (i.e.,) two hours after blending the soil and nano-silica indicated that soil treated with 0.4% of nano-silica showed better performance with an increase in UCS by 25.3%, as seen in Fig. 7. But, as the curing period increased to 7, 14, and 28 and 180 days, soil treated with 0.6% of nano-silica showed better performance with an improvement by 47.4%, 60.4%, 62.9% and 221.4%, respectively, and is therefore considered as the optimum dosage for strength improvement. The trend in the improvement of the strength of the treated soil can be observed from Fig. 7. Thomas and Rangaswamy (2020) reported that the improvement of 1% nano-silica treated soil is 5.09 times and that of 1% cement and 1% nano-silica treated soil is 5.12 times after 28 days of curing. Similarly, based on the results of Ansary *et al.* (2007), for 3% lime and 6% fly ash treated clay the strength improvement is around 4 times higher that of an untreated clay. These improvements offered by heavily dosed lime, cement and fly ash treated clay were almost in the range of strength improvement offered by lower dosage of nano-silica. This indicates that choice of nano-silica as a soil stabilizer is a viable and economic option as a small dosage of nano-silica is adequate compared to the large quantities of conventional cementitious material like lime, cement, and fly ash, etc for strength improvement.

The enhancement in the strength of the treated soil can be attributed to two mechanisms - void plugging by the nano-silica in between silt granules and gel formation upon the reaction between clay, water and nano-silica. Fig. 8 illustrates the mechanism of strength gain through pore filling and formation of viscous gel. Nanomaterials by virtue of their miniscule sizes have large SSA and high surface energy (Ghasabkolaei *et al.* 2017) which enable them to be highly reactive resulting in increased mechanical strength. They form a viscous gel (Changizi and Haddad 2017) by imbibing the water in the soil matrix and enables them to hold the soil particles together inducing strong cohesion resulting in the improvement of strength. The nature of the gel formed and the chemical changes that occur in the soil has also been interpreted through the results of XRD and FTIR analysis.

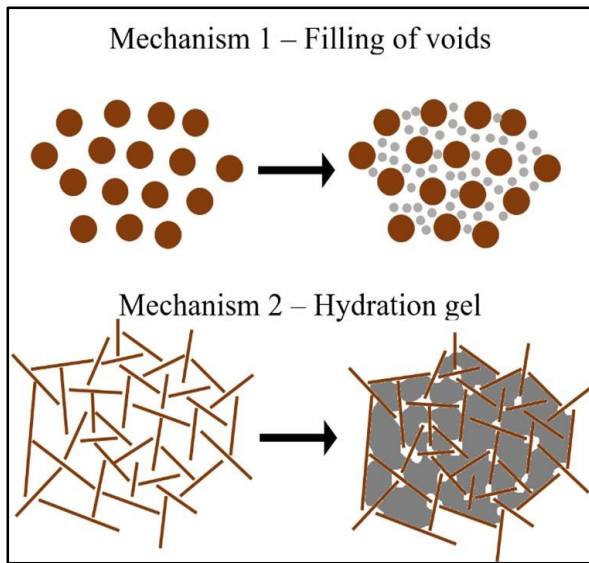


Fig. 8 Mechanisms of strength improvement

Results of the XRD analysis on organic soil and nano-silica treated soil augment the cementing effect of nano-silica. Nano-silica causes the formation of C-S-H owing to the pozzolanic activity of nano-silica particles (Bahmani *et al.* 2014, Ghasabkolaei *et al.* 2017) that results in the increase in compressive strength. XRD analysis was conducted on untreated soil and soil treated with 0.6% of nano-silica. The XRD plots of untreated and 0.6% nano-silica treated soil are shown in Fig. 9. Results of the XRD analysis indicate that the organic soil contains silicon dioxide (SiO_2) and calcium carbonate (CaCO_3) and saponite, a clay mineral that belongs to expansive smectite group which promotes the swelling behaviour in the soil. The 0.6% nano-silica treated soil showed trends matching with calcium silicate hydrate (C-S-H). Hence, the plausible reason behind this improvement in strength could be, the nano-silica and SiO_2 in the untreated soil reacted with the CaCO_3 during hydration forming C-S-H gel. This C-S-H gel helps in the aggregation of soil particles, thereby leading to strength improvement. The reduction in strength at higher dosages (i.e.,) 0.8% in this study can be ascribed to lack of homogenous dispersion due the high SSA and the increase in the amount of nano-particles in the soil matrix (Ghasabkolaei *et al.* 2016) that results in a weak reaction between the soil and nano-silica in the clay matrix. It also inhibits the formation of C-S-H gels (Ghasabkolaei *et al.* 2016) and retards the pozzolanic reaction leading to the reduction in the strength. Ghasabkolaei *et al.* (2016) also reported the formation of unstable and weak lumps at higher dosages leading to reduced strength.

FTIR analysis was conducted to establish the functional group changes upon nano-silica amendment in soil. Fig. 10 depicts the FTIR plot for untreated soil and soil treated with 0.6% nano-silica. The spectral response of the soil showed the presence of clay minerals as observed in the region around 1033 cm^{-1} indicating the alumino-silica lattice of clay minerals like illite, smectite and kaolinite (Tinti *et al.* 2015), thus confirming the presence of saponite in the soil. The slight shift in frequency from 3429 cm^{-1} in organic soil

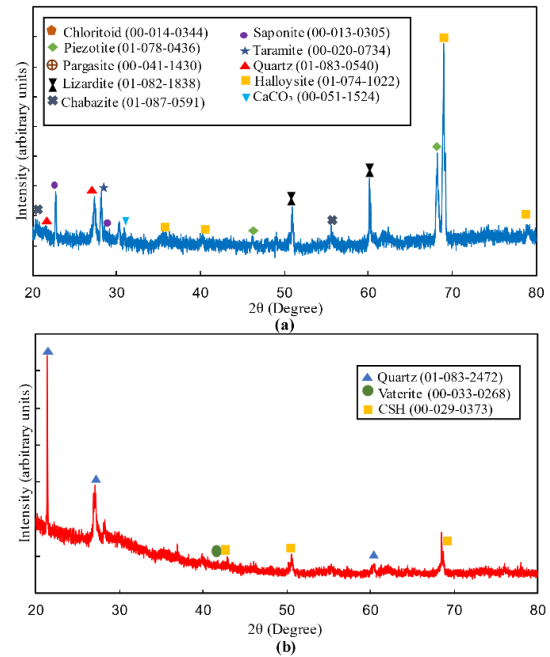


Fig. 9 XRD profile of (a) untreated soil and (b) 0.6% nano-silica treated soil

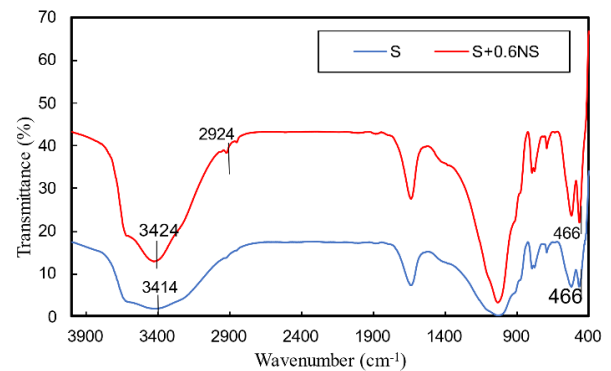


Fig. 10 FTIR profile of untreated soil and nano-silica treated soil

to 3414 cm^{-1} in nano-silica treated soil and the minor change in the shape of the spectral response indicates the stretching of -OH group, which could be due to adsorption of water (Buazar 2019, Vakili *et al.* 2020). The high intensity peak with sudden change in intensity around a frequency of 1033 cm^{-1} indicates stacking of nano-silica and black soil, thereby inferring the formation of C-S-H reaction product (Lv *et al.* 2018).

Fig. 11 depicts the surface roughness profiles obtained by image profilometry analysis of the SEM micrographs presented in Fig. 5. Also, the roughness coefficients obtained from the software analysis are tabulated in Table 5. It can be inferred from Table 5 that there is a marginal increase in the difference of peak and valleys in the profile upon the addition of nano-silica. Despite the varying dosage, the mean roughness of the nano-silica treated soil varies from $0.07\text{ }\mu\text{m}$ to $0.12\text{ }\mu\text{m}$, indicating that the C-S-H gel cements the soil and deters the increase in smoothness of the soil on the outer surface (Fig. 11).

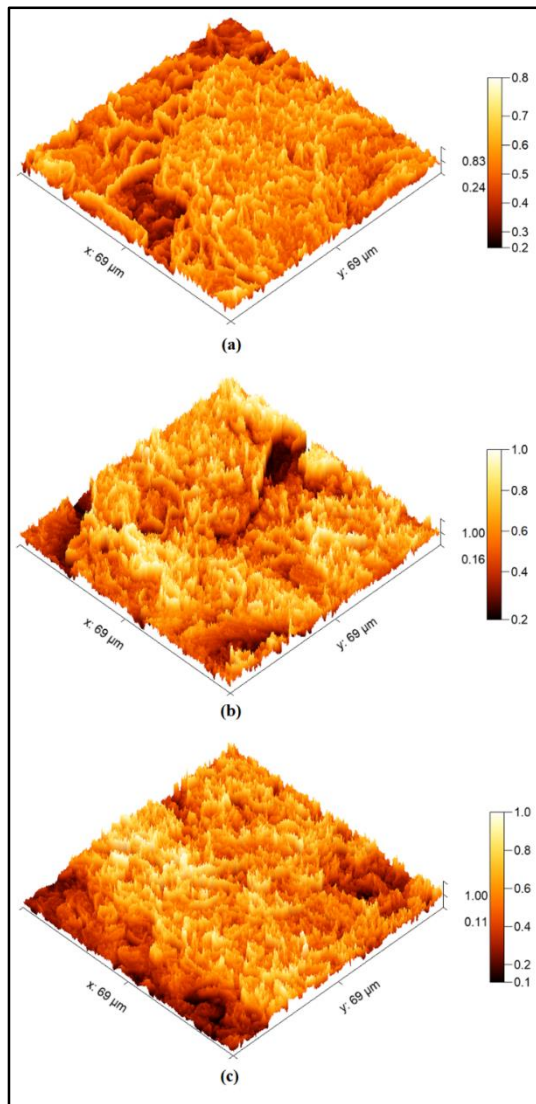


Fig. 11 Surface roughness profiles of (a) S and (b) S+0.6NS (0 day) (c) S+0.8NS (0 day)

Table 5 Results of surface roughness analysis

Sample	Roughness (μm)		
	Sz (Mean of peak and valley)	Sq (Root mean square roughness)	Sa (Mean roughness)
S	0.81	0.10	0.07
S+0.6NS (0 day)	0.84	0.15	0.12
S+0.8NS (0 day)	0.89	0.15	0.12

The increase in roughness can also possibly contribute to the increase in the mechanical strength of nano-silica treated soils by increasing the interlocking between the aggregated particles during loading (Chen *et al.* 2015). However, it should be noted that these image processing results are merely indicative and require additional studies on morphology using better methods like Atomic Force microscopy (AFM) for better interpretation of surface characteristics.

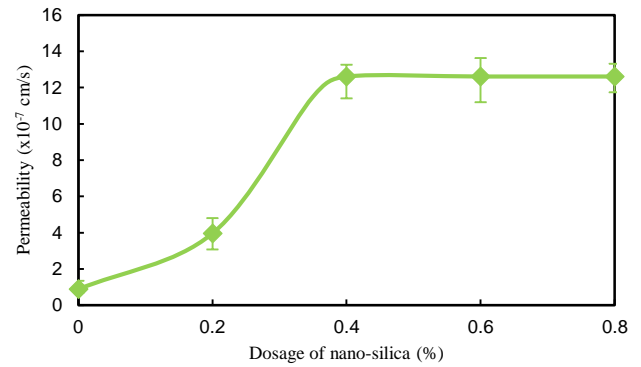


Fig. 12 Variation of permeability at different dosages of nano-silica

Table 6 Results of pore size analysis from image processing technique

Sample	Porosity	Average pore radius
S	0.12	4.13
S+0.6NS (0 day)	0.14	3.85
S+0.8NS (0 day)	0.17	3.37

4.4 Permeability characteristics of nano-silica stabilized soil

Permeability is the measure of the soil mass's ability to allow the infiltration of water into it. Fig. 12 shows the permeability of the soils upon adding various dosages of nano-silica. The permeability of soil increased with an increase in nano-silica dosage. The permeability of organic soil is 8.8×10^{-8} cm/s, upon adding 0.2% and 0.4% of nano-silica, the permeability increased to 4.0×10^{-7} cm/s and 12.6×10^{-7} cm/s respectively. Further, addition of nano-silica to 0.6% and 0.8% did not significantly increase permeability. An almost constant permeability value with a maximum value of 12.6×10^{-7} cm/s was achieved at 0.8% of nano-silica. Treating the soil with nano-silica has led to the flocculation of soil particles resulting in the increase in voids spaces of the soil matrix. As a consequence, the permeability of the soil also increases (Fig. 12). Authors Bahmani *et al.* (2014) also report an increase in permeability of the nano-silica treated soil, particularly at higher dosages. But nanomaterials like nano-clay and colloidal silica have resulted in the decrease in permeability. Kananizadeh *et al.* (2011) reported a decrease in permeability from 3×10^{-9} cm/s to 7.74×10^{-11} cm/s due to the dispersive nature induced on test soil by the nano clay causing a reduction in permeability. Gallagher *et al.* (2007) reported that colloidal silica involves cementing individual grains with each other to form a thick grout like structure on sand, thus reduces the permeability of the sand. Hence this clearly indicates that the nature of soil after gel formation decides the permeability behaviour of the soil.

SEM images from Fig. 5 were analyzed using image processing techniques to quantify the voids ratio at each dosage, estimate soil's porosity and its permeability performance. The results obtained from the image processing technique is tabulated in Table 6. Results indicate that at 0.6 % and 0.8% of nano-silica, the treated

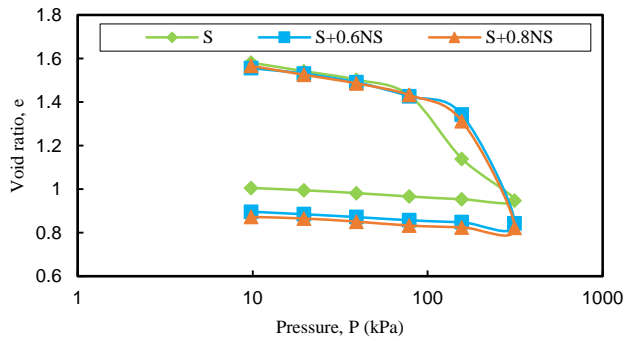


Fig. 13 Compression plot for untreated and nano-silica treated soils

Table 7 Results of consolidation tests

Sample	C_v $\times 10^{-5}$ (cm ² /s)	C_c	C_s	p'_c (kPa)
S	3.666	0.971	0.021	87.100
S+0.6NS	23.986	1.661	0.017	204.170
S+0.8NS	24.021	1.671	0.007	213.790

C_v : Coefficient of consolidation;

C_c : Compression index; C_s : Swell index;

p'_c : pre-consolidation stress

soil's porosity increased compared to the untreated soil. However, the average pore size of 0.6% nano-silica treated soil is remained higher than that of 0.8% treated soil, explaining the relatively smaller pores seen in SEM images of 0.8% treated soil in Fig. 5.

4.5 Compressibility characteristics of nano-silica stabilized soil

Effect of nano-silica on the compressibility of the soil was investigated using the one-dimensional consolidation test. Consolidation tests were conducted on virgin soil and soil blended with 0.6% and 0.8% nano-silica. NYC Building Code (2008) suggests an allowable bearing pressure of 287 kPa on silty type soils. Further, the soil also possesses organic content. Hence a pressure increment of 313.81 kPa was considered for the consolidation studies (Mishra and Das 2012, Katti and Shingote 2019). Fig. 13 depicts the e -log p curves for the tested samples. It is inferred that at lower pressures, the curves exhibited almost similar behaviour, but at higher pressures beyond the 78.45 kPa, the nano-silica treated soil exhibited a different behaviour when compared to untreated soil and the e -log p curve started exhibiting a steeper nature beyond a pressure of 156.91 kPa. Further, the trend of e -log p curve of 0.6% and 0.8% nano-silica treated soil remains almost same, indicating the consolidation behaviour remains almost similar with increase in dosage. Nano-silica increased the compressibility of the soil. An increase of nearly 71% and 72 % was observed on treating the soil with 0.6% and 0.8% nano-silica (Table 7). At lower pressures, negligible change of void ratio was observed in nano-silica treated specimens. However, at higher pressure of 156.91 kPa; the void ratio increased in both 0.6% and 0.8% nano-silica amended soils in comparison with the untreated soil.

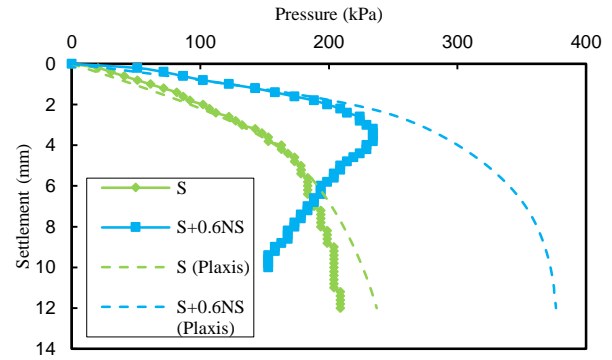


Fig. 14 Pressure-settlement curve from model study and PLAXIS 2D validation

The increase in compressibility can again be attributed to aggregation and subsequent increase in voids as seen from Fig. 5 and table 6. The pre-consolidation stress for untreated soil is 87.10 kPa and it increased with dosage with a maximum of 213.79 kPa for 0.8% nano-silica treated soil. Similar trends on pre-consolidation pressure have been observed by Changizi and Haddad (2017) on nano-silica treated clay. The swell index tends to decrease with the addition of nano-silica and this may be because of the resistance offered by gel formed between the soil particles to particle rearrangement. Based on the results, the coefficient of consolidation for untreated soil, 0.6% and 0.8% nano-silica treated soil are 3.67×10^{-5} cm²/s, 23.99×10^{-5} cm²/s and 24.02×10^{-5} cm²/s. The coefficient of consolidation tends to increase marginally by nearly 5.5 times and reflects the change in permeability of the soil. Results indicate that the rate of consolidation increased with the addition of nano-silica. The addition of nano-silica leads to the aggregation of the soil particles (Lv *et al.* 2018) which results in the increase in the voids between the soil particles causing a rise in the coefficient of consolidation. García *et al.* (2017) worked on nano-silica treated lacustrine clays. They pointed out that compressible floc with surface edge bonds were formed upon nano-silica treatment. With inadequate water these flocs enhanced strength and stiffness. It is inferred that at very high-water content the clay could be susceptible to compression. Further their research indicates that clay content and the nature of clay mineral plays a crucial role in the behavior of the amended soil. Table 6 also points out that, with an increase in nano-silica dosage, the porosity of the sample increased. At the saturated state, the nano-silica treated samples with more voids and higher permeability tend to expel water faster, thereby causing an increase in the consolidation rate at higher dosages with increased pressure.

4.6 Model footing study on nano-silica treated soil

Model foundation study was conducted on untreated soil and on soil treated with 0.6% nano-silica as it yielded the maximum strength improvement during the experimental investigations. The pressure-settlement behaviour for the untreated and treated soil is shown in Fig. 14. Results indicate that the untreated soil experienced failure without

any definite sharp/clear peak at failure. Double tangent method was used to ascertain the load at failure. The double tangent drawn to the pressure-settlement curve of the untreated soil indicates that failure occurred at a pressure of 182 kPa. The trend of the pressure-settlement curve of the 0.6% nano-silica treated soil indicates that the failure was distinct with pattern resembling a general shear failure condition. This could be due to the improvement in the stiffness of the soil upon nano-silica treatment as inferred through the experimental results, where the UCS was 234 kPa at failure and stress-strain response of the UCS test showed a distinct failure load (Fig. 6). The results show that the failure stress from the model study and UCS analysis are in compliance with each other with less than 8% deviation in the values.

Prior to the parametric study, the results of the model study are validated using PLAXIS 2D software to understand the prediction capacity of the software for predicting the results in the actual scenario for such treated soil. Axisymmetric model with mesh and stress distribution contour are shown in Figs. 15(a)-15(c) respectively. PLAXIS validation plots from Fig. 14 indicate that PLAXIS overpredicts the results. This overprediction could be due to the fact that the test was conducted in a simpler 2D axisymmetric environment and also due to the complexity involved in preparing the test soil in the confined test tank environment which would have yielded deviation in the results. A similar case has been explained by Chheng and Likitlersuang (2018) in their study stating that 3D finite element method results would yield better results closer to experimental data and also explained the deviation in results due to the usage of PLAXIS 2D. However, they insisted the point that complexity in calculation and computational time can be effectively reduced in 2D finite element models. Hence, a factor of 0.5 was applied to the PLAXIS based validation in the study to yield results closer to the model study (Chheng and Likitlersuang 2018). Results of validation indicates that the software produced similar trend of curve for untreated soil whereas the trend of failure in nano-silica treated soil with a distinct failure stress was not replicated in the software analysis. However, the trend was similar till failure in both experimental and numerical curves for treated soil. Also, the stress distribution response as seen from Fig. 15(c) indicates that there will be no boundary effect in the study if a similar footing to boundary ratio is adopted.

4.7 Parametric study on nano-silica treated soil

Parametric study was conducted on untreated soil, treated soil with 0.2%, 0.4% and 0.6% of nano-silica. The dosage of 0.8% of nano-silica was ignored as higher strength was obtained from 0.6% nano-silica and using a dosage of 0.8% would yield uneconomical results. Stabilization was done to a depth of 3 m below the footing base with varying dosage in each layer as shown in Table 8. A maximum of three-layer amendment was studied considering the three varying dosages adopted for the study. A variety of guidelines are available for limiting the settlement of the foundation. National Building code of

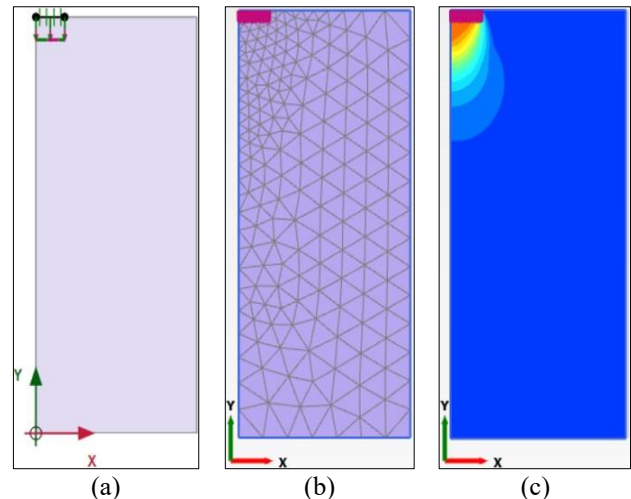


Fig. 15 (a) Axisymmetric loading condition with prescribed displacement (b) Mesh generation and (c) Stress contour

India (2016) suggests a maximum permissible settlement of 75 mm for isolated footing of framed structures on plastic clay. Eurocode accepted a settlement of 50 mm in general for normal structures with isolated footings (BS EN 1997-1 2004). Bangladesh National Building Code (2012) adopted the same guidelines as National Building Code of India (2005), however they suggested that a total settlement 40 mm for isolated pad footings on clay is considered safe. The present study soil has both clay and silt in it with organic content. To attain a uniform comparison of results, a conservative value of load corresponding to 40 mm settlement was taken into account from each analysis. Results from table 8 indicate that soil treated with 0.6% nano-silica for the entire 3 m depth showed improvement nearly 1.1 to 1.3 times for all the footing sizes investigated. But this would yield a comparatively uneconomical solution as 0.6% nano-silica by weight of the soil has to be used for the entire depth of stabilization.

To achieve a cost-effective solution, three cases with near equivalent performance was taken into consideration. First case is, soil treated with 0.6% nano-silica for the top 2.5 m followed by 0.4% addition for the next 0.5 m. Second case is with 0.6% nano-silica treatment for the top 2.5 m of soil and 0.2% addition for the next 0.5 m of soil. The third case is soil treated with 0.6% nano-silica for the top 2.5 m followed by 0.4% addition in the middle 0.25 m and 0.2% nano-silica for the bottom 0.25 m of soil. Despite yielding a comparatively lower performance than treating entirely with 0.6% nano-silica, these three cases produced an economical alternative by reducing the dosage of additive in the subsequent layers. All the three cases produced nearly equivalent results with a deviation around 1.1% with each other. Among the three cases, higher strength was observed in the first case with 0.6% nano-silica addition for the top 2.5 m and 0.4% for the next 0.5 m. But, considering cost as a prime factor, soil treated with 0.6% nano-silica for top 2.5 m followed by 0.2% nano-silica for the next 0.5 m would yield an economical alternative. Although this combination yields lesser strength than treating entire soil with 0.6% nano-silica, it should be noted that it exhibited an uncompromising improvement of around 1.0 to 1.1 times than footing on untreated soil.

Table 8 Numerical results for addition of nano-silica at various layers of soil

No of additive layers	Depth up to which each dosage of nano-silica being used			Load in kN for varied footing size		
	0.6%NS	0.4%NS	0.2%NS	1.2 m	1.5 m	1.8 m
Untreated soil	-	-	-	97.7	130.2	164.8
1 layer	(T)3.0 m	-	-	221.6	274.8	372.3
	-	(T)3.0m	-	173.6	205.4	254.4
	-	-	(T)3.0 m	135.4	151.2	191.9
2 layers	(T)0.5 m	(B)2.5 m	-	182.4	239.0	279.8
	(T)1.0 m	(B)2.0 m	-	206.6	259.0	305.5
	(T)1.5 m	(B)1.5 m	-	188.6	264.2	316.3
	(T)2.0 m	(B)1.0 m	-	205.5	260.2	322.6
	(T)2.5 m	(B)0.5 m	-	206.4	271.2	329.1
	(T)0.5 m	-	(B)2.5 m	161.2	207.6	244.3
	(T)1.0 m	-	(B)2.0 m	192.4	238.5	281.6
	(T)1.5 m	-	(B)1.5 m	188.8	251.8	299.4
	(T)2.0 m	-	(B)1.0 m	202.0	254.2	313.4
	(T)2.5 m	-	(B)0.5 m	205.6	268.5	325.4
3 layers	(T)0.5 m	(M)1.25 m	(B)1.25 m	161.2	232.0	272.0
	(T)1.0 m	(M)1.0 m	(B)1.0 m	202.3	252.4	297.8
	(T)1.5 m	(M)0.75 m	(B)0.75 m	188.9	259.8	310.3
	(T)2.0 m	(M)0.5 m	(B)0.5 m	204.5	257.9	319.1
	(T)2.5 m	(M)0.25 m	(B)0.25 m	206.0	270.0	327.5

T: Top; M: Middle; B: Bottom

5. Conclusions

Experimental studies were conducted to investigate the role of nano-silica in enhancing the performance of organic silt. Nano-silica enhanced the strength of the soil but varied the desired permeability and consolidation characteristics under completely saturated condition. The following conclusion are drawn from the study,

- The liquid limit and plasticity index of the soil increased with the nano-silica. At 0.8% dosage of nano-silica liquid limit and plasticity index increased by 20.9 % and 38.84 % respectively.
- Shrinkage limit also increased with the addition of nano-silica but converged at higher dosages. A maximum rise of 55.22 % is observed at 0.8 % nano-silica addition.
- MDD and OMC decreased with nano-silica treatment. MDD showed a marginal decrease of 4.17% at 0.8% nano-silica. OMC decreased by 20% at the same nano-silica content.
- Stabilizing soil with nano-silica enhanced the strength of the black soil. Initially (0 day) the optimum dosage was 0.4% at which the UCS increased by 25.3%. With passage of time, the optimum dosage increased to 0.6%. At all investigated dosages, strength of nano-silica treated soil remained higher than the untreated soil at all dosages.
- Curing time improved the performance of nano silica treated soil. The strength of the 0.6% nano-silica treated soil increased by 62.9% after 28 days of curing and 221.4% after 180 days of curing.
- SEM, XRD and FTIR studies revealed that hydration of soil and nano-silica mixture formed CSH gel in the soil matrix, which aggregated the soil particles leading to strength improvement
- Nano-silica caused an increase in the permeability of the treated soil. An increase of nearly 13.32 times was observed in the permeability of 0.8 % nano-silica addition. The increase in permeability was due to flocculated behaviour imposed by the nano-silica in the soil mass, thereby increasing the void spaces to facilitate the permeability.
- The compressibility of the soil was not impacted significantly with the addition of nano-silica. The coefficient of consolidation increased by 5.5 times at a dosage 0.8 % nano-silica and the pre-consolidation stress is increased by 1.45 times.
- Practical application for the study has been investigated through model foundation studies. PLAXIS validation indicates that the trend of numerical and experimental analysis are in good agreement until failure, despite the mechanism of shear.
- Parametric studies indicate that, soil treated with 0.6% nano-silica for 3 m below ground level would yield highest performance with 1.1 to 1.3 times improved load carrying capacity for the footing sizes investigated. However, treating soil with 0.6% nano-silica for the top 2.5 m below ground level followed by

0.2% nano-silica treatment for the next 0.5 m would yield a near optimum and economic result with improvement around 1.0 to 1.1 times for all the footings sizes.

Acknowledgments

The authors thank the Vice Chancellor and the management of SASTRA Deemed University, Thanjavur, India for the support and facilities provided to carry out this work successfully.

References

- Ahmadi, H. (2019), "Experimental study of the effect of nano-additives on the stiffness of cemented fine sand", *Int. J. Geotech. Eng.*, <https://doi.org/10.1080/19386362.2019.1663067>.
- Ahmadi, H. and Shafiee, O. (2019), "Experimental comparative study on the performance of nano-SiO₂ and microsilica in stabilization of clay", *Eur. Phys. J. Plus.*, **134**, <https://doi.org/10.1140/epjp/i2019-12918-1>.
- Ali, O.K. and Abbas, H.O., (2019), "Performance assessment of screw piles embedded in soft clay", *Civ. Eng. J.*, **5**(8), 1788-1798. <https://doi.org/10.28991/cej-2019-03091371>.
- Alsharif, J.M.A., Taha, M.R., Firoozi, A.A. and Govindasamy, P. (2016), "Potential of using nanocarbons to stabilize weak soils", *Appl. Environ. Soil Sci.*, <https://doi.org/10.1155/2016/5060531>.
- Ansary, M.A., Noor, M.A. and Islam, M. (2007), "Effect of fly ash stabilization on geotechnical properties of Chittagong coastal soil", *Solid Mech. Appl.*, **146**, 443-454. https://doi.org/10.1007/978-1-4020-6146-2_26.
- ASTM D1194-94 (1994), Standard Test Method for Bearing Capacity of Soil for Static Load and Spread Footings (Withdrawn 2003), ASTM International, West Conshohocken, PA.
- ASTM D427-04 (2004), Method for shrinkage factors of soils by the mercury method (Withdrawn 2008), ASTM International, West Conshohocken, PA.
- ASTM D698 (2012), Standard test methods for laboratory compaction characteristics of soil using standard effort (12 400 ft-lbf/ft³ (600 kN-m/m³)), ASTM International, West Conshohocken, PA.
- ASTM D2166 / D2166M (2016), Standard test method for unconfined compressive strength of cohesive soil, ASTM International, West Conshohocken, PA.
- ASTM D5856 (2015), Standard test method for measurement of hydraulic conductivity of porous material using a rigid-wall, compaction-mold permeameter, ASTM International, West Conshohocken, PA.
- ASTM D2487 (2017), Standard practice for classification of soils for engineering purposes (Unified Soil Classification System), ASTM International, West Conshohocken, PA.
- ASTM D4318 (2017), Standard test methods for liquid limit, plastic limit, and plasticity index of soils, ASTM International, West Conshohocken, PA.
- ASTM D5890 (2019), Standard test method for swell index of clay mineral component of geosynthetic clay liners, ASTM International, West Conshohocken, PA.
- ASTM D2435 / D2435M (2020), Standard test methods for one-dimensional consolidation properties of soils using incremental loading, ASTM International, West Conshohocken, PA.
- ASTM D2974 (2020), Standard test methods for determining the water (moisture) content, ash content, and organic material of peat and other organic soils, ASTM International, West Conshohocken, PA.
- Bahmani, S.H., Farzadnia, N., Asadi, A. and Huat, B.B.K. (2016), "The effect of size and replacement content of nanosilica on strength development of cement treated residual soil", *Constr. Build. Mater.*, **118**, 294-306. <https://doi.org/10.1016/j.conbuildmat.2016.05.075>.
- Bahmani, S.H., Huat, B.B.K., Asadi, A. and Farzadnia, N. (2014), "Stabilization of residual soil using SiO₂ nanoparticles and cement", *Constr. Build. Mater.*, **64**, 350-359. <https://doi.org/10.1016/j.conbuildmat.2014.04.086>.
- Bahrami, R., Khayat, N. and Nazarpour, A. (2020), "Effect of nano-stabilizer on geotechnical properties of leached gypsiferous soil", *Geomech. Eng.*, **23**(2), 103-113. <https://doi.org/10.12989/gae.2020.23.2.103>.
- Bangladesh National Building Code (2015), Volume 2, Part 6, Bangladesh.
- Bobet, A., Hwang, J., Johnston, C.T. and Santagata, M. (2011), "One-dimensional consolidation behavior of cement-treated organic soil", *Can. Geotech. J.* **48**(7), 1100-1115. <https://doi.org/10.1139/t11-020>.
- BS EN 1997-1 (2004), Eurocode 7: Geotechnical design—Part 1: General rules.
- Buazar, F. (2019), "Impact of Biocompatible Nanosilica on Green Stabilization of Subgrade Soil", *Sci. Rep.*, **9**. <https://doi.org/10.1038/s41598-019-51663-2>.
- Changizi, F. and Haddad, A. (2017), "Improving the geotechnical properties of soft clay with nano-silica particles", *Proc. Inst. Civ. Eng. Gr. Improv.*, **170**(2), 62-71. <https://doi.org/10.1680/jgrim.15.00026>.
- Changizi, F. and Haddad, A. (2015), "Strength properties of soft clay treated with mixture of nano-SiO₂ and recycled polyester fiber", *J. Rock Mech. Geotech. Eng.*, **7**(4), 367-378. <https://doi.org/10.1016/j.jrmge.2015.03.013>.
- Chen, X., Zhang, J., Xiao, Y. and Li, J. (2015), "Effect of roughness on shear behavior of red clay-concrete interface in large-scale direct shear tests", *Can. Geotech. J.*, **52**(8), 1122-1135. <https://doi.org/10.1139/cgj-2014-0399>.
- Chheng, C. and Likitlersuang, S. (2018), "Underground excavation behaviour in Bangkok using three-dimensional finite element method", *Comput. Geotech.* **9**, 68-81. <https://doi.org/10.1016/j.compgeo.2017.09.016>.
- Choobasti, A.J. and Kutanaei, S.S. (2017), "Microstructure characteristics of cement-stabilized sandy soil using nanosilica", *J. Rock Mech. Geotech. Eng.*, **9**(5), 981-988. <https://doi.org/10.1016/j.jrmge.2017.03.015>.
- Choobasti, A.J., Samakoosh, M.A. and Kutanaei, S.S. (2019), "Mechanical properties soil stabilized with nano calcium carbonate and reinforced with carpet waste fibers", *Constr. Build. Mater.*, **211**, 1094-1104. <https://doi.org/10.1016/j.conbuildmat.2019.03.306>.
- Dash, S.K., Sireesh, S and Sitharam, T.G. (2003), "Microstructure characteristics of cement-stabilized sandy soil using nanosilica", *Geotext. Geomembranes.*, **21**(4), 197-219. [https://doi.org/10.1016/S0266-1144\(03\)00017-7](https://doi.org/10.1016/S0266-1144(03)00017-7).
- Erzin, Y. and Gunes, N. (2013), "The unique relationship between swell percent and swell pressure of compacted clays", *Bull. Eng. Geol. Environ.*, **72**, 71-80. <https://doi.org/10.1007/s10064-013-0461-z>.
- Ezeakacha, C.P., Rabbani, A., Salehi, S. and Ghalambor, A. (2018), "Integrated image processing and computational techniques to characterize formation damage", *Proc. - SPE Int. Symp. Form Damage Control*, Louisiana, February. <https://doi.org/10.2118/189509-ms>.
- Firoozi, A.A., Olgun, C.G., Firoozi, A.A. and Baghini, M.S. (2017), "Fundamentals of soil stabilization", *Int. J. Geo-Eng.*, **8**. <https://doi.org/10.1186/s40703-017-0064-9>.

- Gallagher, P.M., Pamuk, A. and Abdoun, T. (2007), "Stabilization of Liquefiable Soils Using Colloidal Silica Grout", *J. Mater. Civ. Eng.*, **19**, 33-40. [https://doi.org/10.1061/\(asce\)0899-1561\(2007\)19:1\(33\)](https://doi.org/10.1061/(asce)0899-1561(2007)19:1(33)).
- Gao, L., Ren, K., Ren, Z. and Yu, X. (2018), "Study on the shear property of nano-MgO-modified soil", *Mar. Georesour. Geotechnol.*, **36**(4), 465-470. <https://doi.org/10.1080/1064119X.2017.1335813>.
- García, S., Trejo, P., Ramírez, O., Molina, J.L. and Hernández, N. (2017), "Influence of Nanosilica on compressive strength of lacustrine soft clays", *Proceedings of the 19th International Conference on Soil Mechanics and Geotechnical Engineering*, Seoul, South Korea, September.
- Ghadr, S., Langroudi, A.A., Hung, C., O'Kelly, B.C., Bahadori, H. and Ghodsi, T. (2020), "Stabilization of sand with colloidal nanosilica hydrosols", *Appl. Sci.*, **10**(15). <https://doi.org/10.3390/app10155192>.
- Ghadr, S., Assadi-Langroudi, A. and Hung, C. (2020), "Stabilisation of peat with colloidal nanosilica", *Mires. Peat.*, **26**. <https://doi.org/10.19189/MaP.2019.OMB.StA.1896>.
- Ghasabkolaei, N., Janalizadeh, A. and Jahanshahi, M. (2016), "Physical and geotechnical properties of cement-treated clayey soil using silica nanoparticles: An experimental study", *Eur. Phys. J. Plus.*, **131**. <https://doi.org/10.1140/epjp/i2016-16134-3>.
- Ghasabkolaei, N., Choobbasti, A.J., Roshan, N. and Ghasemi, S.E. (2017), "Geotechnical properties of the soils modified with nanomaterials: A comprehensive review", *Arch. Civ. Mech. Eng.*, **17**(3), 639-650. <https://doi.org/10.1016/j.acme.2017.01.010>.
- Ghazavi, M. and Bolhasani, M. (2010), "Unconfined compression strength of clay improvement with lime and nano-silica", *Proceedings of the 6th International Congress on Environmental Geotechnics*, New Delhi, November.
- Ghazi, H. (2011), "The effects of Nano-material additives on the basic properties of soil", *Proceedings of the 14th Asian Regional Conference on Soil Mechanics and Geotechnical Engineering*, China, May.
- Gupta, D. and Kumar, A. (2017), "Stabilized soil incorporating combinations of rice husk ash, pond ash and cement", *Geomech. Eng.*, **12**(1), 85-109. <https://doi.org/10.12989/gae.2017.12.1.085>.
- Hidalgo, C., Carvajal, G. and Muñoz, F. (2019) "Laboratory evaluation of finely milled brick debris as a soil stabilizer", *Sustain.*, **11**(4). <https://doi.org/10.3390/su11040967>.
- Ijimdiyaa, T.S., Ashimiyu, A.L. and Abubakar, D.K. (2012) "Stabilization of black cotton soil using groundnut shell ash", *Electron. J. Geotech. Eng.*, **17**, 3645-3652.
- Kananzadeh, N., Ebadi, T., Khoshniat, S.A. and Mousavirizi, S.E. (2011), "The Positive Effects of Nanoclay on the Hydraulic Conductivity of Compacted Kahrizak Clay Permeated with Landfill Leachate", *Clean - Soil Air Water*, **39**(7), 605-611. <https://doi.org/10.1002/clen.201000298>.
- Karthick, S., Muralidharan, S., Lee, H.S., Kwon, S.J. and Saraswathy, V. (2019), "Reliability and long-term evaluation of GO-MnO₂ nano material as a newer corrosion monitoring sensor for reinforced concrete structures", *Cement Concrete Compos.*, **100**, 74-84. <https://doi.org/10.1016/j.cemconcomp.2019.03.012>.
- Katti, A.R. and Shingotte, S.B. (2019), "Laboratory study on consolidation settlement of foundation on soft saturated marine clay overlain by geocells infilled with sand", *Proceedings of Indian Geotechnical Conference 2019*, Surat, India, December.
- Krishnan, J. and Shukla, S. (2019), "The behaviour of soil stabilised with nanoparticles: an extensive review of the present status and its applications", *Arab. J. Geosci.*, **12**. <https://doi.org/10.1007/s12517-019-4595-6>.
- Luo, H.L., Hsiao, D.H., Lin, D.F. and Lin, C.K. (2012), "Cohesive Soil Stabilized Using Sewage Sludge Ash/Cement and Nano Aluminum Oxide", *Int. J. Transp. Sci. Technol.*, **1**(1), 83-99. <https://doi.org/10.1260/2046-0430.1.1.83>.
- Lv, Q., Chang, C., Zhao, B. and Ma, B. (2018), "Loess Soil Stabilization by Means of SiO₂ Nanoparticles", *Soil. Mech. Found. Eng.*, **54**, 409-413. <https://doi.org/10.1007/s11204-018-9488-2>.
- Mishra, D.P. and Das, S.K. (2012), "One-dimensional consolidation of sedimented stowed pond ash", *Geotech. Geol. Eng.*, **30**, 685-695. <https://doi.org/10.1007/s10706-011-9486-x>.
- Mohanty, S.K., Pradhan, P.K. and Mohanty, C.R. (2017), "Stabilization of expansive soil using industrial wastes", *Geomech. Eng.*, **12**(1), 111-125. <https://doi.org/10.12989/gae.2017.12.1.111>.
- National Building Code of India (2005), Group 2, Part 6, New Delhi, India.
- Norhasri, M.S.M., Hamidah, M.S. and Fadzil, A.M. (2017), "Applications of using nano material in concrete: A review", *Constr. Build. Mater.*, **133**, 91-97. <https://doi.org/10.1016/j.conbuildmat.2016.12.005>.
- NYC Building Code (2014), Chapter 18, Section 1804, New York.
- Pavlović, Ž., Risović, D. and Novaković, D. (2012). "Comparative study of direct and indirect image-based profilometry in characterization of surface roughness", *Surf. Interface Anal.*, **44**(7), 825-830. <https://doi.org/10.1002/sia.4889>.
- Qu, X., Alvarez, P.J.J. and Li, Q. (2013), "Applications of nanotechnology in water and wastewater treatment", *Water. Res.*, **47**(12), 3931-3946. <https://doi.org/10.1016/j.watres.2012.09.058>.
- Rabbani, A. and Salehi, S. (2017), "Dynamic modeling of the formation damage and mud cake deposition using filtration theories coupled with SEM image processing", *J. Nat. Gas. Sci. Eng.*, **42**, 157-168. <https://doi.org/10.1016/j.jngse.2017.02.047>.
- Rastegarnia, A., Alizadeh, S.M.S., Esfahani, M.K., Amini, O. and Utyuzh, A.S. (2020), "The effect of hydrated lime on the petrography and strength characteristics of Illite clay", *Geomech. Eng.*, **22**(2), 143-152. <https://doi.org/10.12989/gae.2020.22.2.143>.
- Sadoglu, E., Cure, E., Moroglu, B. and Uzuner, B.A. (2009), "Ultimate loads for eccentrically loaded model shallow strip footings on geotextile-reinforced sand", *Geotext. Geomembranes*, **27**(3), 176-182. <https://doi.org/10.1016/j.geotexmem.2008.11.002>.
- Sakr, M.A., Shahin, M.A. and Metwally, Y.M. (2009), "Utilization of lime for stabilizing soft clay soil of high organic content", *Geotech. Geol. Eng.*, **27**, 105-113. <https://doi.org/10.1007/s10706-008-9215-2>.
- Saloma, Nasution, A., Imran, I. and Abdullah, M. (2015), "Improvement of concrete durability by nanomaterials", *Procedia Eng.*, **125**, 608-612. <https://doi.org/10.1016/j.proeng.2015.11.078>.
- Shahsavani, S., Vakili, A.H. and Mokhberi, M. (2020), "The effect of wetting and drying cycles on the swelling-shrinkage behavior of the expansive soils improved by nanosilica and industrial waste", *Bull. Eng. Geol. Environ.*, **79**, 4765-4781. <https://doi.org/10.1007/s10064-020-01851-6>.
- Shooshpasha, I. and Shirvani, R.A. (2015), "Effect of cement stabilization on geotechnical properties of sandy soils", *Geomech. Eng.*, **8**(1), 17-31. <https://doi.org/10.12989/gae.2015.8.1.017>.
- Sikora, P., Elrahman, M.A. and Stephan, D. (2018), "The influence of nanomaterials on the thermal resistance of cement-based composites—A review", *Nanomater.*, **8**(7), 1-33. <https://doi.org/10.3390/nano8070465>.
- Tabarsa, A., Latifi, N., Meehan, C.L. and Manahiloh, K.N. (2018), "Laboratory investigation and field evaluation of loess improvement using nanoclay – A sustainable material for construction", *Constr. Build. Mater.*, **158**, 454-463. <https://doi.org/10.1016/j.conbuildmat.2017.09.096>.
- Taha, M.R., Alsharef, J.M.A., Khan TA, Aziz, M and Gaber, M (2018), "Compressive and tensile strength enhancement of soft soils using nanocarbons", *Geomech. Eng.*, **16**(5), 559-567. <https://doi.org/10.12989/gae.2018.16.5.559>.

- Taha, M.R. and Ying, T. (2018), "Effects of carbon nanotube on kaolinite: basic geotechnical behavior", *Proceedings of the 18th Annual International Conference on Composites/Nano Engineering*, Alaska, July.
- Taha, M.R. and Taha, O.M.E. (2012), "Influence of nano-material on the expansive and shrinkage soil behavior", *J. Nanoparticle Res.* **14**. <https://doi.org/10.1007/s11051-012-1190-0>.
- Tastan, E.O., Edil, T.B., Benson, C.H. and Aydilek, A.H. (2011), Stabilization of organic soils with fly ash, *J. Geotech. Geoenviron. Eng.*, **137**(9), 819-833. [https://doi.org/10.1061/\(asce\)gt.1943-5606.0000502](https://doi.org/10.1061/(asce)gt.1943-5606.0000502).
- Tejasvi, A. and Kumar, S. (2012), "Impact of fly ash on soil properties", *Natl. Acad. Sci. Lett.*, **35**, 13-16. <https://doi.org/10.1007/s40009-011-0002-x>.
- Thomas, G. and Rangaswamy, K. (2020), "Strengthening of cement blended soft clay with nano-silica particles", *Geomech. Eng.*, **20**(6), 505-516. <https://doi.org/10.12989/gae.2020.20.6.505>.
- Tinti, A., Tugnoli, V., Bonora, S. and Francioso, O. (2015), "Recent applications of vibrational mid-infrared (IR) spectroscopy for studying soil components: A review", *J. Cent. Eur. Agric.*, **16**(1), 1-22. <https://doi.org/10.5513/JCEA01/16.1.1535>.
- Vakili, A.H., Shojaei, S.I., Salimi M, Selamat, M.R.B. and Farhadi, M.S. (2020), "Contact erosional behaviour of foundation of pavement embankment constructed with nanosilica-treated dispersive soils", *Soils Found.*, **60**(1), 167-178. <https://doi.org/10.1016/j.sandf.2020.02.001>.
- Wong, C., Pedrotti, M., Mountassir, G.E. and Lunn, R.J. (2018), "A study on the mechanical interaction between soil and colloidal silica gel for ground improvement", *Eng. Geol.*, **243**, 84-100. <https://doi.org/10.1016/j.enggeo.2018.06.011>.